Draft version February 28, 2022
Typeset using LaTeX **twocolumn** style in AASTeX63

Parameter estimation with non stationary noise in gravitational waves data

Sumit Kumar,[1,2] Alexander H. Nitz,[1,2] and Xisco Jiménez Forteza[1,2]

[1] *Max-Planck-Institut für Gravitationsphysik (Albert-Einstein-Institut), D-30167 Hannover, Germany*
[2] *Leibniz Universität Hannover, D-30167 Hannover, Germany*

ABSTRACT

The sensitivity of gravitational-waves detectors is characterized by their noise curves which determine the detector's reach and the ability to accurately measure the parameters of astrophysical sources. The detector noise is typically modelled as stationary and Gaussian for many practical purposes. However, physical changes in the state of detectors due to environmental and instrumental factors, including extreme cases where a detector discontinues observing for some time, introduce non-stationarity into the noise. Even slow evolution of the detector sensitivity will affect long duration signals such as binary neutron star (BNS) mergers. Mis-estimation of the noise behavior directly impacts the posterior width of the signal parameters. This becomes an issue for studies which depend on accurate localization volumes such as i) probing cosmological parameters (such as Hubble constant, clustering bias) using cross-correlation methods with galaxies, ii) doing electromagnetic follow-up using localization information from parameter estimation done from pre-merger data. We study the effects of dynamical noise on the parameter estimation of the GW events. We develop a new method to correct dynamical noise by estimating a locally-valid pseudo PSD which is normalized along the time-frequency track of a potential signal. We do simulations by injecting the BNS signal in various scenarios where the detector goes through a period of non-stationarity with reference noise curve of third generation detectors (Cosmic explorer, Einstein telescope). As an example, for a source where mis-modelling of the noise biases the signal-to-noise estimate by even 10%, one would expect the estimated localization volume to be either under or over reported by $\sim 30\%$; errors like this, especially in low-latency, could potentially cause follow-up campaigns to miss the true source location.

Keywords: gravitational waves — power spectral density —binary neutron stars — third generation detectors

1. INTRODUCTION

Since the first detection of gravitational waves (GW) from the merger of two compact objects in 2015 (Abbott et al. 2016), GW science has come a long way and GW detections have become a routine (Abbott et al. 2021a; Nitz et al. 2021b). LIGO observatories in Livingston and Hanford (Aasi et al. 2015) have already finished three science runs, namely O1, O2, and O3 (Abbott et al. 2021a). The GW observatories: Virgo (Acernese et al. 2015) in Italy and KAGRA in Japan (Akutsu et al. 2021) joined the LIGO-Hanford and LIGO-Livingston observatories in O2 and O3 respectively. Currently, there are more than 90 confident GW detections from the merger of compact objects as identified by various data analysis pipelines summed up as GWTC-3 catalog (Abbott et al. 2021a) and 4-OGC catalog (Nitz et al. 2021b). In the upcoming decade, the network of ground base GW detectors is set to be expanded with the addition of LIGO-India (Saleem et al. 2022). The current ground base detectors are also set to undergo phases of improvement in sensitivity (Abbott et al. 2018). Additionally, the proposed third generation of ground based detectors (Shoemaker et al. 2021) such as the Einstein telescope (ET) (Sathyaprakash et al. 2012), and Cosmic Explorer (CE) (Reitze et al. 2019; Evans et al. 2021) are expected to have an order of magnitude better sensitivity and will be able to probe lower gravitational-wave frequencies ($f_{low} \sim 3 - 5$ Hz). This will help in rapidly expanding the gravitational-wave catalog.

The ever growing catalog enables us to answer important questions about the intrinsic population properties

Corresponding author: Sumit Kumar
sumit.kumar@aei.mpg.de

of the sources; these include the mass function, spin distribution, and redshift distribution (Abbott et al. 2021b). By inferring the localization volumes of individual GW merger events with the help of parameter estimation (PE) methods, and by cross correlating the localization volumes with galaxy catalogs, one can also estimate the cosmological parameters such as the Hubble constant (Abbott et al. 2021c), and large scale distribution of matter (Vijaykumar et al. 2020; Mukherjee et al. 2021a; Libanore et al. 2021; Mukherjee et al. 2021b; Caas-Herrera et al. 2021). The reach of third-generation detectors also implies a large population of loud BNS mergers which will be prime candidates for electromagnetic-followup campaigns. It will also feasible to infer the sky location from the early part of the signal and alert the electromagnetic (EM) telescope before a merger and the subsequent electromagnetic emission occurs (Chan et al. 2018; Nitz & Dal Canton 2021). The correct estimation of the localization volumes requires accurately understanding and modelling the noise of the detector along with the signals.

Data from the GW detectors is analysed using the time series strain data $s(t)$ which might contain a signal $h(t)$ and the detector noise $n(t)$. The noise is typically assumed to be Gaussian, stationary, and colored. This makes it easy to model the noise.

In GW searches, the data is analyze in chunks and the the power spectral density (PSD) of the noise is typically estimated for a segment of data $\sim 256 - 1024$s using Welch's method (Abbott et al. 2020; Usman et al. 2016). It is assumed that the PSD is constant during this time. This PSD is then used to calculate the signal-to-noise ratio (SNR) ρ by applying matched filtering to the data for a bank of template waveforms (Allen et al. 2012). Whenever ρ is obtained above a certain threshold, it is called a single detector trigger. The local trigger density depends on the the PSD and if a local deviation from the average PSD is not taken into account, it can affect the estimation of the local trigger density (Mozzon et al. 2020).

For parameter estimation, the estimated PSD is used to calculate the likelihood function and the PSD is assumed to be constant during the time of the signal in the detector frequency band. Again, any significant local time variation from the estimated PSD will affect the likelihood function and therefore affect the width of the posterior and hence the reported uncertainties in the marginalized distribution of individual parameters. For the current generation detectors, we do not expect this bias to be statistically significant for loud signals because most of the signals are short lived ($\sim \mathcal{O}(1-10)$ seconds for BBH and $\sim \mathcal{O}(100)$ seconds for BNS) in the detector sensitivity band. But for third generation detectors, because of the better sensitivity at low frequencies, we expect the signals to be lasting for $\sim \mathcal{O}(100-60000)$ seconds. Due to very long signal durations, any change in noise characteristics due to evolution in the state of the detectors will cause the noise to be non-stationary; modelling the non-stationarity is needed to ensure the most accurate source localization and parameter estimates. An important aspect of long duration signals is that a fraction of them can be identified from few minutes to few hours before the merger can be identified and located in sky with localization information (Nitz & Dal Canton 2021). This can be used to alert various telescopes to point in right direction to be ready for observing the electromagnetic follow-up observations. A mis-estimation of localization volume for pre-merger alert will end up in either wasting telescope time and resources (in case of over estimated localization volume) or in worst case scenario missing out on observing the event (under estimated localization volume).

In this paper we explore the modeling of non-stationary noise and it's implications on parameter estimation. We introduce an efficient method to account for non-stationarity which is slowly varying compared to the signal evolution. This is accomplished by calculating a corrected PSD along the track of the signal by dividing the time-frequency track of a signal into shorter duration segments and estimating a local PSD for each time bin separately. The corrected PSD can be constructed by selecting the frequency range from each local PSD estimate corresponding to the expected signal contribution in the same time range. This method of estimating the PSD depends on getting a preliminary constraint from searches for trigger parameters to identify the track of the signal.

2. GRAVITATIONAL WAVES DATA ANALYSIS

The signal from the merger of two compact objects: binary black holes (BBHs), binary neutron stars (BNS), or neutron star-Black hole (NSBH), as seen in detector, consists of a time series $h(t)$ buried in the noisy data of the detector $n(t)$.

$$s(t) = \begin{cases} n(t) + h(t), & \text{When signal is present} \\ n(t), & \text{otherwise} \end{cases} \tag{1}$$

The shape of the signal $h(t)$ depends on the intrinsic parameters of the source such as the component masses $(m_{1,2})$, the component spins $(s_{1x,2x}, s_{1y,2y}, s_{1z,2z})$ as well as on the extrinsic parameters such as the luminosity distance to the source (D_L), the inclination angle of the

binary to line of sight (ι), the polarization angle (ψ), the coalescence phase (ϕ), the sky localization (right ascension: RA, declination: dec). The noise $n(t)$ has contributions from many sources such as quantum noise, thermal noise, Newtonian noise, and transient noise of unknown origins (Abbott et al. 2020). The overall noise is typically described as a stochastic process modelled as a Gaussian distribution:

$$p(\mathbf{n}) = \frac{1}{\sqrt{2\pi|C_{ij}|}} \exp\left(\frac{1}{2}\sum_{i,j}(n_i-\mu)C_{ij}^{-1}(n_j-\mu)\right) \tag{2}$$

Where $\mathbf{n}$ is a time series vector of a certain noise realization with a given sample rate. μ is the expectation value of the noise and C_{ij} is the covariance between i^{th} and j^{th} bin in the time series. Both these quantities can be estimated from the data. The noise is said to be stationary if the covariance matrix C_{ij} only depend on the lag between bins i and j i.e. $|t_i - t_j|$. A useful property of stationary noise is that the covariance matrix takes a positive diagonal form in frequency domain i.e. $C_{ij} = \delta_{ij} S_n(f_i)$. Here $S_n(f_i)$ is defined as power spectral density which is the Fourier transform of the correlation function $C(\tau)$ where $\tau = |t_i - t_j|$ is the time lag. The validity of the assumptions of the noise being Gaussian and stationary can be tested by various techniques, for example, with large number of injections in simulated Gaussian noise and detector data, the percentile-percentile test is done with posterior samples to see if the recovered credible intervals matches with the statistical expectations (Kulkarni & Capano 2021). One can also use the distribution of PSD variation statistic v_s to identify the stretches of the data which do not agree with the expected statistical distribution of v_s for the Gaussian and stationary noise (Mozzon et al. 2020), or by measuring the noise covariance of the data (Edy et al. 2021).

2.1. *Effects of estimated PSD on the infered signal properties*

The signal to noise ratio (SNR) of a signal template h is defined as $\rho \equiv \frac{(s|h)}{\sqrt{(h|h)}}$ where the inner product $(a|b)$ between two time series $a(t)$ and $b(t)$ (and their counterpart in Fourier domain $a(f)$ and $b(f)$) is defined as:

$$(a|b) \equiv 2\int_{-\infty}^{\infty} \frac{a(f)b^{\star}(f)}{S_n(|f|)}, \tag{3}$$

where, $S_n(f)$ is the estimated power spectrum of the noise over a chosen time window. The GW searches construct the SNR time series to identify a signal in the data. Whenever a template is found to have SNR greater than a pre-defined threshold, it is stored as a single detector trigger. These single detector triggers are then passed through a 'coincidence test' where only those triggers, which are within the light travel time (plus few milliseconds to account for errors in estimating trigger time) between the two detectors, survive. As the estimation of SNR depends on estimated PSD $S_n(f)$, mis-estimation of PSD, will have an effect on the SNR and hence on the trigger density. There are methods available to correct for these effects at the level of the searches, such as applying a psd drift correction (Zackay et al. 2021) and applying dynamic normalization using the PSD variation statistic (Mozzon et al. 2020). However, note that both methods assume a constant change in the overall amplitude of the noise and that this is constant over the duration of the signal. We may expect this to be a reasonable assumption for short-duration signals.

For the parameter estimation, we describe the signal $h(\theta)$ in terms of parameters θ of the waveform model and perform Bayesian analysis to obtain the posterior distribution $p(\theta|d)$ which represents the probability distribution over the parameters θ given the observed data d and model,

$$p(\theta|d) = \frac{\mathcal{L}(d|\theta)\pi(\theta)}{p(d)}, \tag{4}$$

where $\mathcal{L}(d|\theta)$ is the likelihood function: the probability of obtaining the data given the parameter θ describing model. $\pi(\theta)$ is the prior probability distribution for the parameters, and $p(d)$ is known as Bayesian evidence or marginalized likelihood which acts as normalization factor. For the Gaussian noise model, the likelihood function in the frequency domain takes the form:

$$\mathcal{L} \propto \exp\left(-\frac{1}{2}n^{\star}(f)S_n^{-1}(f)n(f)\right). \tag{5}$$

As shown in (Edy et al. 2021), the effects of mis-estimating the PSD can be calculated by doing a linear series expansion of the waveform template h around the true signal value h_0. The mis-estimation of the $S_n(f)$ only results in over (or under) estimating the posterior width. In other words, if we use two different estimates of $S_n(f)$, the posteriors will still be centred at the same values but the width of the posteriors will be different. Specifically, at linear order in the signal h_0, the covariance matrix of the waveform parameters – the inverse of the Fisher matrix (Vallisneri 2008) – scales linearly with $S_n(f)$, while the SNR of the signal as $S_n^{-1}(f)$. Thus, as a rule of thumb, a PSD variation of type $S_n(f) \to \alpha S_n(f)$ – a variation of the noise floor – will broaden/narrow the width on the posterior distributions of the physical parameters by the same factor

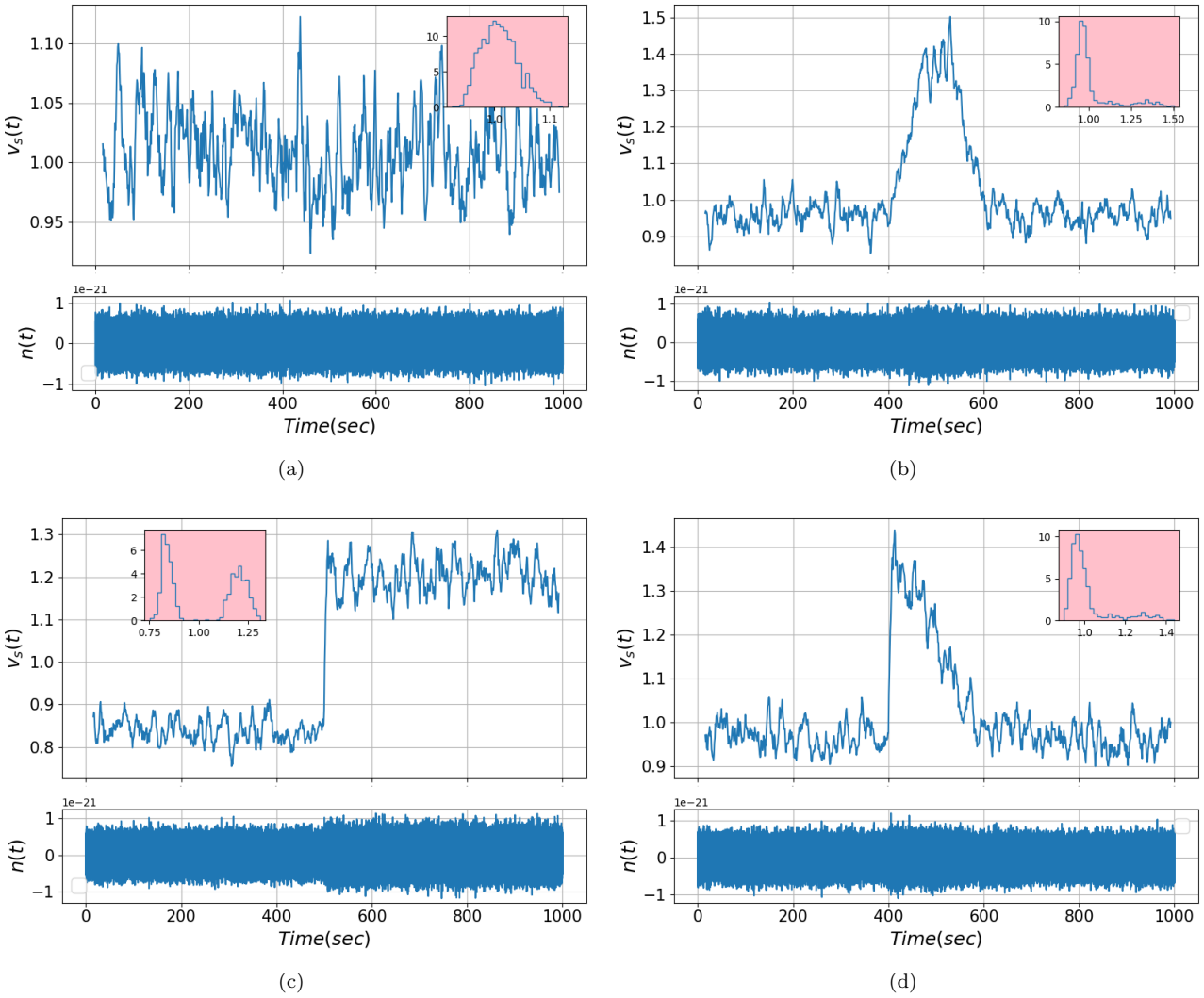

Figure 1. Different types of local variation in the PSD are considered here. To track the local variation in PSD, we use the PSD variation statistic v_s described in (Mozzon et al. 2020). In all the figures, the lower panel shows the strain data for 1000 seconds. Top panel shows the local PSD variation statistic with respect to the PSD estimated for the entire duration (1000 seconds). In the inset, the distribution of all the PSD variation values is shown. Different scenarios of non-stationarities considered in these figures are: (a) Baseline noise model with Gaussian and stationary assumptions. The local variations in the PSD are due to the Gaussian random fluctuations. (b) The baseline noise model is acted upon by a filter with a bump in the middle. We use $B(t) = B_0 sin(\frac{\pi}{\Delta T} t)$ with $[B_0, \Delta T] = [0.2, 200sec]$ so that it produces a bump in the amplitude of positive half sine wave between t=400 to t=600 seconds. (c) The floor of the baseline PSD is lifted in the middle (at t=500 seconds) with $B(t) = 0.2$ for $t >$ 500sec (d) The floor of the PSD is lifted at t=400 second and drops down to the base scale slowly in due time by t=600 seconds.

α, which results in increasing their inferred uncertainty. This may become very relevant for the studies where the localization volumes are very important, such as i) pre-merger localization, ii) estimating Hubble parameter using cross correlation methods with galaxy catalogs, and iii) probing large scale structures using two point correlation function of localization volumes with next generation GW detectors. For all the studies mentioned above, the estimation of correct localization volume is important for unbiased estimators. In a study by Mozzon et al. (2021), through simulation of BNS signals, it is shown that though non-stationary noise will not be a limiting factor for resolving Hubble tension for current generation of detectors, it will play important roll for 3G detectors. On the other hand, the non-stationary models considered are not expected to introduce any bias on the estimated parameters at least at linear order (Edy et al. 2021).

If the data is non-stationary, the covariance matrix in the frequency domain also contains the off diagonal el-

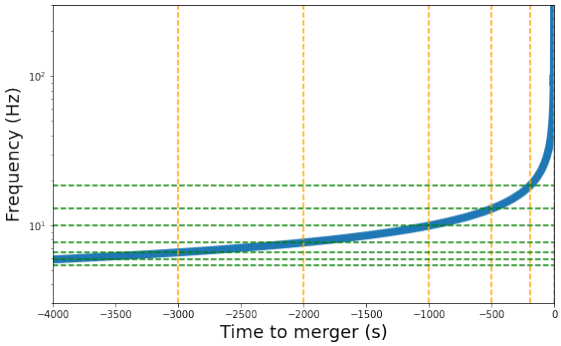

Figure 2. We show a frequency-time track of a GW signal from the merger of binary neutron star. The track of the signal can be used to identify the times corresponding to the frequency bins to estimate the PSD of the noise.

ements and the estimation of the likelihood function 5 becomes computationally expensive. So it is difficult to just model the non-stationarities in a straight forward way without compromising the computational costs. In one of the studies, (Edy et al. 2021) shows that it is important to account for the non-stationarity in the signals that lasts longer than few minutes such as BNS signals in current detectors and BBH/BNS signals in third generation GW detectors.

3. ESTIMATING LOCAL VARIATION IN THE PSD

To check for the stationarity of the data, one can estimate the noise covariance. One can also use other methods such as PSD variation statistics described in (Mozzon et al. 2020). The non-stationarity of the data will lead to difference in actual power spectrum $S_A(f)$ and estimated one $S_E(f)$ modelled with the help of PSD variation statistics v_s,

$$S_A(f) = v_s S_E(f) \tag{6}$$

where $S_E(f)$ is the estimated power spectral density over long stretch of data using the Welch method with smaller overlapping segments. Using a filter $\mathcal{F}(f) = \frac{h(f)}{S_E(f)}$, with approximating $|h(f)| \propto f^{-7/6}$ (dominant amplitude behaviour of the CBC signal during the inspiral phase), v_s can be estimated by computing the convolution between the data $s(f)$ and filter $\mathcal{F}(f)$.
The non-stationarity in the detector noise can be attributed to various factors of known or unknown origin. There are different non-stationary noise models considered in the literature (Vajente et al. 2020; Hebbal et al. 2019; Edy et al. 2021). A few examples are:

- **local fluctuations in the detector noise due to non stationary component:** It might be the case that there is some non-stationary component in the overall noise. This can be modelled as follows: $n(t) = An_1(t) + B(t)n_2(t)$ (Edy et al. 2021). Here the first component $n_1(t)$ is stationary Gaussian noise and second component $n_2(t)$ represents noise of unknown origin with a time-dependent component $B(t)$. A special case of above is when the noise is Gaussian but the overall amplitude varies as a function of time such that $n(t) = (1 + B(t))A_0 n_1(t)$.
- **A shift in the overall PSD:** There are times when detector goes out of lock and comes back online but with overall noise floor raised above the reference PSD and slowly comes back to the more stable configuration.

In figure 3, we show some examples of the types of non-stationarities described above. We use a baseline noise model (Gaussian, stationary colored noise) and apply a filter upon it to scale the amplitude of Gaussian noise as function of time according to desired non stationary nature. This may not be the most general way to model the non-stationarity but we consider it to test our correction method in parameter estimation. We use PSD variation statistic v_s to track the non-stationary nature of the noise. For the examples shown in the figure, we generated $\sim$ 1000 seconds of data with Gaussian noise with one of the available noise model 'aLIGOZeroDetHighPower' in the publicly available software package LALSuite (LIGO Scientific Collaboration 2018). We call this baseline noise model. For the baseline model, the local PSD variation is due to purely Gaussian random fluctuations so the PSD variation statistic v_s have mean around $< v_s >= 1$ with standard deviation consistent with that of the Gaussian fluctuations. We generate the non stationary noise by applying a filter on baseline noise such that the amplitude of the Gaussian noise varies as desired function. This type of PSD variation can be modelled as,

$$n(t) = (1 + B(t))A_0 n_G(t) \tag{7}$$

where $A_0 n_G(t)$ is the stationary, Gaussian, colored noise, $B(t)$ models the variation in the amplitude. $B(t) = 0$ corresponds to the baseline noise model. As shown in figure 3, we introduce some arbitrary non-stationarity in the noise at various times and use PSD variation statistics v_s to track it.

4. MODELING THE NON-STATIONARITY FOR PARAMETER ESTIMATION

In most of the standard parameter estimation (PE) pipelines, to obtain the posterior distribution 4, a sampling method (such as MCMC, nested sampling) is used

Table 1. The description of various scenarios of non stationary noise considered. We use noise sensitivity curve for Cosmic Explorer design sensitivity (Hall et al. 2021) with low frequency cutoff of $f_{low} = 5Hz$. The non-stationarity in the noise is introduced by applying a filter the baseline noise model with a time varying amplitude for a fixed time window. To estimate the SNR, we estimate the PSD by two methods: i) Using a long segment of 8000 seconds surrounding the trigger time t_c, using Welch's method by dividing the whole segment into smaller chunks of 8 seconds. And ii) Estimated along the frequency-time track of the reference BNS signal. The PSD estimated along the track of the signal is used as reference to estimate fractional difference in SNR $= |\delta\rho|/\rho_{\rm ref}$.

S. No.	Amplitude variation	Description	SNR difference (%)
1.	$B(t) = \begin{cases} B_0, & : t > t_{shift} \\ 0, & : \text{otherwise} \end{cases}$	A positive shift, described by a step function, in the amplitude of the Gaussian noise at $t_{shift} = t_c - 190$ seconds. $B_0 = 0.8$, and t_c is the trigger time of the signal. Therefore the signal spend last 190 seconds (before merger) buried in the noise characterized by, where noise floor is raised according to the equation.	43.6
2.	$B(t) = \begin{cases} -\frac{B_0}{\Delta T}(t - t_1) + B_0, & : t_1 < t < t_1 + \Delta T \\ 0, & : \text{otherwise} \end{cases}$	A positive shift in the amplitude of the noise followed by a linear decay to original amplitude (base scale). We use $B_0 = 0.8$, $\Delta T = 600$ seconds, and $t_1 = t_c - 650$. The signal spent 600 seconds of time in non stationary noise where the noise floor was above the base scale.	11.47
3.	$B(t) = \begin{cases} B_0 \sin\left(\frac{\pi(t-t_1)}{\Delta T}\right), & : t_1 < t < t_1 + \Delta T \\ 0, & : \text{otherwise} \end{cases}$	A bump described by a half positive cycle of sine function with $B_0 = 0.8$, $\Delta T = 600$ seconds, and $t_1 = t_c - 650$. The signal spend 600 seconds of time in non-stationary noise where noise floor was lifted above the base scale.	21.19
4.	$B(t) = \begin{cases} B_0, & : t < t_{shift} \\ 0, & : \text{otherwise} \end{cases}$	A drop in the amplitude of the Gaussian noise at $t_{shift} = t_c - 10$ seconds. $B_0 = 0.8$, and t_c is the trigger time of the signal. So the signal spend all the time until 10 seconds prior to the merger in the noise characterized by where noise floor is raised with respect to base scale.	9.11

with a likelihood model and prior probability distribution over the model parameters. The PSD is estimated for a segment of the data around the signal using the Welch's method with smaller overlapping segments or spline-modelling such as implemented by the Bayesline algorithm (Littenberg & Cornish 2015). For example, to estimate the PSD for PE in 4OGC and 3OGC analysis (Nitz et al. 2021b,a), 512 seconds of data centered around trigger is used to estimate the PSD with overlapping segments of 8 seconds (unless the data is corrupted in this window, in which case, this window is shifted and/or shrunk). The estimated PSD is then used in the calculation of likelihood function 5. The averaged PSD over the long segment surrounding the signal wash away any local fluctuations (or non-stationarities) that might be present along the track of the signal. In order to incorporate the non-stationarity, one has re-define the likelihood function by incorporating non diagonal terms in covariance matrix estimated in frequency domain.

In this work, we propose a new method to model certain types of non-stationarities where the strain data can be divided into smaller chunks of "stationary" or "semi-stationary" parts: such as slowly varying Gaussian noise amplitude, sudden lift or drop in the noise floor, even

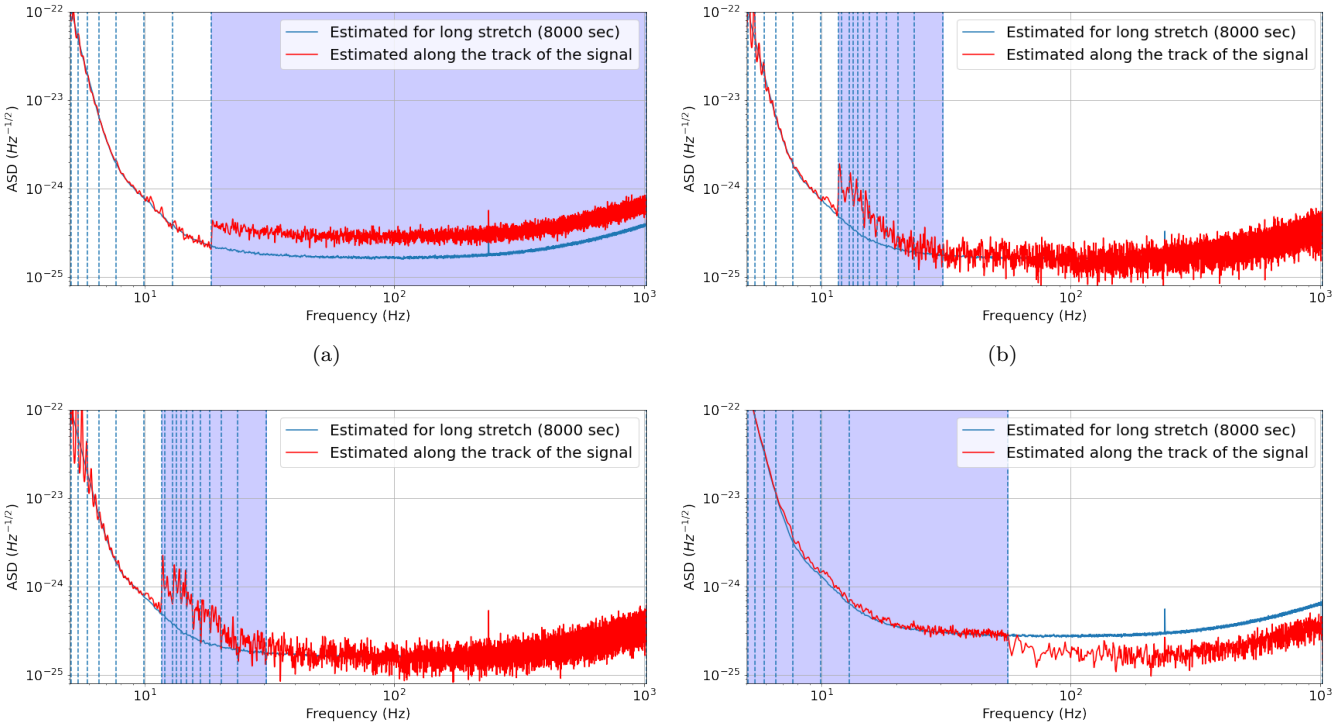

Figure 3. The estimated amplitude spectral density (ASD) as a function of frequency. The blue curve represents the the ASD estimated for long segment (8000 seconds) around the signal and red curve represent the ASD estimated along the track of the signal as described in the text. We inject the BNS signal in the non stationary noise as described in the Table 1. The shaded region represents the frequency range along the track of the signal when detector went through the period of non stationary noise. During this time, the noise amplitude is increased as a function of time. This is reflected in the raised (estimated) noise floor. The figures (a),(b),(c), and (d) corresponds to the scenarios (1),(2),(3), and (4) in the table 1 respectively

missing some duration of data (for example detector being offline) for very long duration signals. For 3G GW detectors such as Einsteins Telescope (ET) or cosmic explorer (CE), due to their low frequency reach, the BBH signals can be $\sim \mathcal{O}(100) - \mathcal{O}(1000)$ seconds long and BNS signals can be $\sim \mathcal{O}(1000) - \mathcal{O}(60000)$ seconds long depending on the value of low frequency cutoff. During this time, it is possible that detector goes through periods of non-stationarities. Even for the current generation detectors, a BNS signal in the detector band is usually few hundred seconds long. When the track of the signal in detector band is long enough, we can estimate the PSD along the track of the signal. To do so, we can use reference signal parameters obtained from the searches as trigger with maximum SNR. The track of the reference signal can be drawn in the frequency-time graph and it can be broken in frequency bins (and corresponding time bin). We can then estimate the PSD for each frequency bins by using strain data from corresponding time bin and stack the estimated PSD in each frequency bin to estimate a corrected PSD along the track of the signal. In figure 2, we show frequency time track of a reference BNS signal. We divide the track of the signal in frequency-time graph into smaller bins. We assume that the variations in the detector noise across each time (frequency) bins are negligible so that we can model the detector noise in each bin to be Gaussian and stationary.

In Table 1, we show various scenarios of arbitrary non stationary noise we considered in simulations. We inject a BNS signal with parameters ($m_{1,source} = 1.5M_\odot$, $m_{2,source} = 1.3M_\odot$, $D_L = 100$ Mpc) in the data such that the detector goes through a period of non-stationarity during the course of the signal. We estimate the SNR using two estimated PSDs: i) assuming the detector noise is constant during the signal and estimating average PSD from long stretch of data around signal, and ii) estimating PSD along the track of the signal as described above. We estimate the fractional SNR difference ($\frac{\delta_\rho}{\rho}$) arising from two PSDs and found that there can be significant fractional SNR difference (upto $\sim 40\%$) for the arbitrary non stationary noise we consider here. In reality, these differences might not be as extreme but even a few percent difference in fractional

SNR will have an effect on localization volumes. We use the baseline noise model from the design sensitivity of 3G detector cosmic explorer. We use 3G detector noise curve only for the reason that BNS signals are expected to last for very long time in the detector frequency band. The current method can be applied to current detectors as well when we see the non-stationarity (similar to ones considered in the examples) along the track of a long BNS signal lasting few hundred seconds.

In figure 3, we show the estimated PSD in both ways for all the injection scenarios described in table 1. The frequency and time bins are chosen such that the local variation in the PSD can be tracked.

4.1. *Simulations and Parameter Estimation*

To put this method to test, we inject a GW signal from the merger of a BNS ($m_{1,source} = 1.5M_\odot$, $m_{2,source} = 1.3M_\odot$, $D_L = 100$ Mpc) in a network of third generation gravitational wave detector. We consider two cosmic explorer (CE) detectors (one located in USA and other in Australia), and Einstein telescope (ET) (Europe). We summarize the properties of the detector network in Table 2. The CE is proposed to be built in two phases, known as CE1 and CE2 (Hall et al. 2021), with second phase having better sensitivity. We consider the design sensitivity for both the detectors. E_1, E_2, and E_3 in our notation denote the three effetively independent detectors that make up the ET observatory. We choose 3G detector network to demonstrate the differences solely because it is very likely for signals to be present when detector undergoes the non stationary times. The methods described here will be applicable to any scenario with long duration signals where the data can be divided into smaller chunks of stationary (or semi stationary) times to estimate the PSD along the track of the signal.

In the 3G detector network we considered, we introduce arbitrary non-stationarities modelled in 7 as follows:

- CE^U: We introduce non-stationarity described by a step function $B(t) = B_0$ for $t > t_c - 180$ seconds,i.e. noise floor is raised around 180 seconds before the trigger time t_c.
- CE^A: Here we introduce the non-stationarity in the detector noise by dropping the noise floor of the detector at base level 10 seconds prior to the trigger time. Mathematically, $B(t) = B_0$ for $t < t_c - 10$.
- E_1: In this detector we again used positive step function $B(t) = B_0$ for $t > t_c - 50$ seconds.
- E_2: Noise floor drops to base scale 50 seconds prior to trigger time: $B(t) = B_0$ for $t < t_c - 50$.

We do not introduce any non-stationarity in the detector E_3. We use $B_0 = 0.8$ for this simulation. Notice that all these non-stationarities will have different effect in the fractional SNR difference of the detector network.

We do Bayesian parameter estimation, using publicly available code PyCBC Inference (Biwer et al. 2019). We use uniform priors in detector frame chirp mass $\mathcal{M}$, mass ratio $(q = m_1/m_2); m_1 >= m_2$, comoving volume, and time of arrival t_c. We use the isotropic prior for RA, dec, inclination angle, and polarization. We use TaylorF2 waveform model (Blanchet et al. 1995; Faye et al. 2012) implemented in LALSuite (LIGO Scientific Collaboration 2018) to simulate the signal to be injected in the noise, and for recovery while doing parameter estimation. To estimate the likelihood function, we make use of the heterodyne likelihood model described in (Cornish 2010; Finstad & Brown 2020; Zackay et al. 2018). To reduce the computational costs, we use the sample rate of 1024 to generate the data. We use low frequency cutoff $f_{low} = 5.1$ Hz for $CE^{U,A}$ and $f_{low} = 5$Hz for ET, and high frequency cutoff $f_{high} = 512$ Hz for all detectors to estimate likelihood function.
In figure 4, we show the difference in the localization volume inferred from two methods of estimating the PSD. It shows the difference localization volumes for two cases. The difference in network SNR corresponding to maximum likelihood obtained for this example is 4.76%.

5. SUMMARY AND DISCUSSION

The current methods of parameter estimation (PE) using GW data assume stationary noise. Estimation of the PSD over a large chunk of data washes away any local fluctuations due to any possible non-stationarity in the data. The stationary noise has a useful property that the correlation function of time series between two times t_1 and t_2 depends only on the time difference $|t_1 - t_2|$. In the frequency domain, it means that the covariance matrix is diagonal. These assumptions help in simplifying the likelihood function and make it faster to calculate. If any non-stationarity is present in the data and not accounted for, it will not primarily shift estimates of source parameters, but will most directly affect width of the posterior distributions and hence reported errors on parameters. A simple method to incorporate (any) non stationarity present in the data is to estimate the off diagonal terms in the likelihood function 5. While exact, this makes the estimation of the likelihood function impractically expensive for most purposes.

Table 2. The specifications of 3G detector network (location, low frequency cutoff $f_{\rm low}$) considered in this study. We use the design sensitivity noise curves for ET and CE. These detectors configuration for CE and ET are also used in previous work (Hall & Evans 2019; Nitz & Dal Canton 2021; Kumar et al. 2021)

Abbreviation	Observatory	$f_{\rm low}$	Latitude	Longitude
CE^U	Cosmic Explorer USA	5.2	40.8	-113.8
CE^A	Cosmic Explorer Australia	5.2	-31.5	118.0
E	Einstein Telescope	5	43.6	10.5

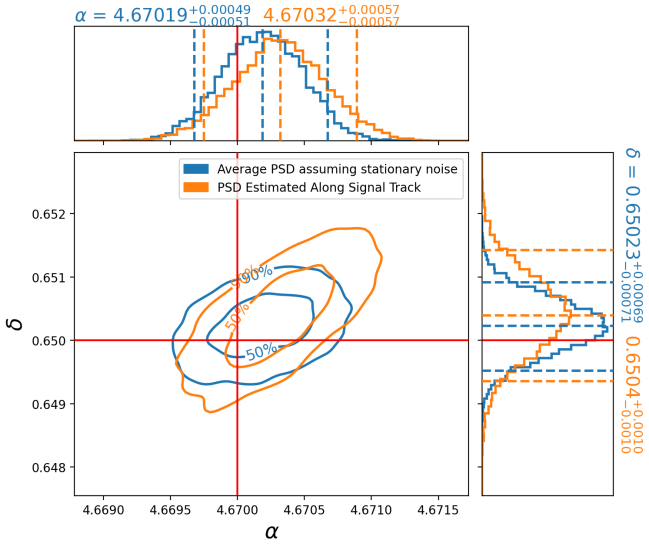

Figure 4. This figure shows difference in localization volume for right ascension and declination angle arising for two cases. Blue contours represents the 50% and 90% credible intervals when an constant PSD is used for parameter estimation. The orange contours represents same when a PSD estimated along the track of the signal is used The red lines represents the injected values. For this simulation, we used a loud BNS injection ($m_{1,source}$: 1.5 $M_\odot$, $m_{2,source}$: 1.3 $M_\odot$, d_L : 100Mpc) in a third generation detector network of two cosmic explorer and Einstein telescope. See text for the details of detector network and types of non-stationarity considered.

In this work, propose a fast method to incorporate the non stationarity specially for the long signals such as BNS. We propose to estimate the PSD along the track of the signal in the frequency-time graph. We assume that the data can be broken into smaller chunks where it can be assumed to be stationary or semi stationary (such as slowly varying amplitude of the Gaussian noise). We do simulations by injecting a long BNS signal in various scenarios of arbitrary non stationary noise with 3G detectors and show that there there will be difference in the SNR estimated if these effects ts are not accounted for. We also show that it will lead to the difference in estimated localization volume obtained from parameter estimation.

This method is reliable for the types of non-stationarities where the strain data can be broken into piece-wise smaller segments of semi-stationary data such as when amplitude of the Gaussian noise is changing slowly in the smaller time bins. It also relies on identifying nearly the right track of the signal in frequency-time graph. In practice, identifying this track should not be problematic; several bootstrapping schemes are practical, including using the initial point estimates for the coalescence time and chirp mass from standard compact-binary searches.

We note that mis-characterization of the noise also has an effect not-only on the estimation of signal parameters but also on the detection of distance sources due to the mis-estimation of a signal's SNR. The method for calculating a corrected PSD can also be efficiently applied to searches by a simple two-step procedure. In the first stage, an average PSD is used to calculated an initial SNR estimate and identify potential candidates. Once the initial candidates are identified, the SNR can be re-weighted using the corrected PSD. This is natural extension of the dynamic normalization outlined in Mozzon et al. (2020).

We present this as method to incorporate certain types of non-stationarities in the data for parameter estimation. For future work, we plan to modify this method to incorporate more general types of non-stationarities by estimating the PSD along the track of the signal using PSD variation statistic. We also plan to apply this method to study non-stationarities present in the data from the current detectors by identifying those stretches and doing PE by performing BNS injections.

ACKNOWLEDGMENTS

We acknowledge the Max Planck Gesellschaft. We thank the computing team from AEI Hannover for their significant technical support. SK thanks members of Observational relativity and cosmology group at AEI for feedback and useful comments. SK also thanks Aditya Vijaykumar for feedback.

REFERENCES

Aasi, J., et al. 2015, Class. Quant. Grav., 32, 074001, doi: 10.1088/0264-9381/32/7/074001

Abbott, B., Abbott, R., Abbott, T., et al. 2016, Physical Review D, 93, doi: 10.1103/physrevd.93.122003

Abbott, B. P., et al. 2018, Living Rev. Rel., 21, 3, doi: 10.1007/s41114-020-00026-9

Abbott, B. P., Abbott, R., Abbott, T. D., et al. 2020, Classical and Quantum Gravity, 37, 055002, doi: 10.1088/1361-6382/ab685e

Abbott, R., et al. 2021a. https://arxiv.org/abs/2111.03606

—. 2021b, Astrophys. J. Lett., 913, L7, doi: 10.3847/2041-8213/abe949

—. 2021c. https://arxiv.org/abs/2111.03604

Acernese, F., et al. 2015, Class. Quant. Grav., 32, 024001, doi: 10.1088/0264-9381/32/2/024001

Akutsu, T., et al. 2021, PTEP, 2021, 05A101, doi: 10.1093/ptep/ptaa125

Allen, B., Anderson, W. G., Brady, P. R., Brown, D. A., & Creighton, J. D. E. 2012, Phys. Rev. D, 85, 122006, doi: 10.1103/PhysRevD.85.122006

Biwer, C. M., Capano, C. D., De, S., et al. 2019, Publ. Astron. Soc. Pac., 131, 024503, doi: 10.1088/1538-3873/aaef0b

Blanchet, L., Damour, T., Iyer, B. R., Will, C. M., & Wiseman, A. G. 1995, Phys. Rev. Lett., 74, 3515, doi: 10.1103/PhysRevLett.74.3515

Caas-Herrera, G., Contigiani, O., & Vardanyan, V. 2021, The Astrophysical Journal, 918, 20, doi: 10.3847/1538-4357/ac09e3

Chan, M. L., Messenger, C., Heng, I. S., & Hendry, M. 2018, Phys. Rev. D, 97, 123014, doi: 10.1103/PhysRevD.97.123014

Cornish, N. J. 2010. https://arxiv.org/abs/1007.4820

Edy, O., Lundgren, A., & Nuttall, L. K. 2021, Physical Review D, 103, doi: 10.1103/physrevd.103.124061

Evans, M., et al. 2021. https://arxiv.org/abs/2109.09882

Faye, G., Marsat, S., Blanchet, L., & Iyer, B. R. 2012, Class. Quant. Grav., 29, 175004, doi: 10.1088/0264-9381/29/17/175004

Finstad, D., & Brown, D. A. 2020, Astrophys. J. Lett., 905, L9, doi: 10.3847/2041-8213/abca9e

Hall, E. D., & Evans, M. 2019, Classical and Quantum Gravity, 36, 225002, doi: 10.1088/1361-6382/ab41d6

Hall, E. D., et al. 2021, Phys. Rev. D, 103, 122004, doi: 10.1103/PhysRevD.103.122004

Hebbal, A., Brevault, L., Balesdent, M., Talbi, E.-G., & Melab, N. 2019, Bayesian Optimization using Deep Gaussian Processes. https://arxiv.org/abs/1905.03350

Kulkarni, S., & Capano, C. D. 2021, On the reliability of parameter estimates in the first observing run of Advanced LIGO. https://arxiv.org/abs/2011.13764

Kumar, S., Vijaykumar, A., & Nitz, A. H. 2021. https://arxiv.org/abs/2110.06152

Libanore, S., Artale, M. C., Karagiannis, D., et al. 2021, JCAP, 02, 035, doi: 10.1088/1475-7516/2021/02/035

LIGO Scientific Collaboration. 2018, LIGO Algorithm Library - LALSuite, free software (GPL), doi: 10.7935/GT1W-FZ16

Littenberg, T. B., & Cornish, N. J. 2015, Phys. Rev. D, 91, 084034, doi: 10.1103/PhysRevD.91.084034

Mozzon, S., Ashton, G., Nuttall, L. K., & Williamson, A. R. 2021, Does non-stationary noise in LIGO and Virgo affect the estimation of H_0? https://arxiv.org/abs/2110.11731

Mozzon, S., Nuttall, L. K., Lundgren, A., et al. 2020, Classical and Quantum Gravity, 37, 215014, doi: 10.1088/1361-6382/abac6c

Mukherjee, S., Wandelt, B. D., Nissanke, S. M., & Silvestri, A. 2021a, Phys. Rev. D, 103, 043520, doi: 10.1103/PhysRevD.103.043520

Mukherjee, S., Wandelt, B. D., & Silk, J. 2021b, Mon. Not. Roy. Astron. Soc., 502, 1136, doi: 10.1093/mnras/stab001

Nitz, A. H., Capano, C. D., Kumar, S., et al. 2021a, The Astrophysical Journal, 922, 76, doi: 10.3847/1538-4357/ac1c03

Nitz, A. H., & Dal Canton, T. 2021, The Astrophysical Journal Letters, 917, L27, doi: 10.3847/2041-8213/ac1a75

Nitz, A. H., Kumar, S., Wang, Y.-F., et al. 2021b, 4-OGC: Catalog of gravitational waves from compact-binary mergers. https://arxiv.org/abs/2112.06878

Reitze, D., et al. 2019, Bull. Am. Astron. Soc., 51, 035. https://arxiv.org/abs/1907.04833

Saleem, M., et al. 2022, Class. Quant. Grav., 39, 025004, doi: 10.1088/1361-6382/ac3b99

Sathyaprakash, B., et al. 2012, Class. Quant. Grav., 29, 124013, doi: 10.1088/0264-9381/29/12/124013

Shoemaker, D. H., et al. 2021. https://arxiv.org/abs/2112.12718

Usman, S. A., et al. 2016, Class. Quant. Grav., 33, 215004, doi: 10.1088/0264-9381/33/21/215004

Vajente, G., Huang, Y., Isi, M., et al. 2020, Phys. Rev. D, 101, 042003, doi: 10.1103/PhysRevD.101.042003

Vallisneri, M. 2008, Phys. Rev. D, 77, 042001, doi: 10.1103/PhysRevD.77.042001

Vijaykumar, A., Saketh, M. V. S., Kumar, S., Ajith, P., & Choudhury, T. R. 2020. https://arxiv.org/abs/2005.01111

Zackay, B., Dai, L., & Venumadhav, T. 2018.

https://arxiv.org/abs/1806.08792

Zackay, B., Venumadhav, T., Roulet, J., Dai, L., & Zaldarriaga, M. 2021, Physical Review D, 104, doi: 10.1103/physrevd.104.063034